Available online at www.sciencedirect.com
SCIENCE DIRECT
Journal of Power Sources 150 (2005) 120–128
JOURNAL OF POWER SOURCES
www.elsevier.com/locate/jpowsour

Investigation of membrane property and fuel cell behavior with sulfonated poly(ether ether ketone) electrolyte: Temperature and relative humidity effects

Ruichun Jiang [a,*], H. Russell Kunz [a], James M. Fenton [a,b]

[a] *Department of Chemical Engineering, University of Connecticut, Storrs, CT, USA*
[b] *Florida Solar Energy Center, University of Central Florida, Cocoa, FL, USA*

Received 14 February 2005; received in revised form 2 March 2005; accepted 2 March 2005
Available online 31 May 2005

Abstract

Sulfonated poly(ether ether ketone)s (SPEEKs) with various sulfonation degrees were prepared and characterized for the intention of fuel cell applications. Two distinct water vapor activity regions characterized by different water vapor uptake behaviors were observed. Proton conductivity of SPEEK membranes increases with increasing sulfonation degrees and temperatures. SPEEK membranes with sulfonation degrees of 51 and 60% show proton conductivity higher than 0.01 S cm^{-1} at temperatures higher than 40 °C with 100% relative humidity (RH). Relative humidity has a stronger effect on the proton conductivity of SPEEK membranes than that of Nafion® membranes. Fuel cell performance with SPEEK membranes was studied at various temperatures and relative humidities. Good fuel cell performance was obtained with a SPEEK-51 membrane at 80 °C, 100% relative humidity and ambient pressure. Both temperature and relative humidity have important influence to the cell resistances and performances. Cyclic voltammetry (CV) as well as hydrogen crossover profiles show distinct features under different relative humidity conditions.

Keywords: Sulfonated poly(ether ether ketone) (SPEEK); Water vapor uptake; Proton conductivity; Fuel cell performance; Temperature; Relative humidity

1. Introduction

Fuel cells are electrochemical devices that directly convert chemical energy from fuel oxidation into electrical energy. The proton exchange membrane fuel cell (PEMFC), which uses a polymer membrane as an electrolyte, is regarded as highly attractive for generating clean and efficient power for stationary and mobile applications. The proton exchange membrane (PEM) is a key component in the system since that membrane acts as an electrolyte for transferring protons from the anode to the cathode as well as providing a barrier to the passage of electrons and gas crossover between the electrodes. PEM materials should possess the following characteristics: high ionic conductivity (usually > 0.01 S cm^{-1}); high thermal, mechanical and chemical stability under fuel cell operating conditions; low fuel and oxidant permeability; and low cost [1]. Currently, the most commonly used membranes for both hydrogen and direct methanol fuel cells are perfluorinated copolymers such as Nafion®, which has high mechanical and chemical stability and excellent proton conductivity. However, the application of Nafion® membranes has important drawbacks: high cost; loss of conductivity at low relative humidity; and high methanol permeability in direct methanol fuel cells [1–3].

Widespread effort is underway to develop alternative, more economical, non-perfluorinated polymer PEMs for fuel cells. Many promising aromatic thermoplastic polymers, such as poly(aryl ether ketone)s (e.g. PEK, PEEK and PEKK), poly(ether sulfone) (PES), polybenzimidazole (PBI), etc., have excellent chemical, mechanical and thermo-oxidative stability and are low cost. By introducing sulfonic

* Corresponding author. Tel.: +1 860 486 3606; fax: +1 860 486 2959.
E-mail address: rcjiang@engr.uconn.edu (R. Jiang).

0378-7753/$ – see front matter © 2005 Elsevier B.V. All rights reserved.
doi:10.1016/j.jpowsour.2005.03.180

groups or doping phosphoric acid to the polymers' chains, these materials gain proton conductivity and show promising properties as PEMs in fuel cells [4–11]. Several studies have been reported on sulfonated poly(ether ether ketone) (SPEEK) used as a PEM material in both hydrogen and direct methanol fuel cells [12–16]. In addition, blend polymer membranes [17–19] and organic–inorganic membranes [20–23] with SPEEK as the major component have been explored with the goal to obtain good mechanical properties, high proton conductivity, and optimized membrane properties.

Although several studies on SPEEK as fuel cell PEM were previously conducted, some important characterizations, such as membrane water uptake in vapor phase water, temperature and relative humidity effects on cell resistance, membrane water management and fuel cell performance have not been adequately studied. These subjects are the topic of this paper. Investigations of sulfonation control, thermal stability, FTIR study and proton conductivity are also performed and presented.

2. Experimental

2.1. Sulfonation reaction: PEEK → SPEEK

Victrex® PEEK (450PF), provided by Victrex US, Inc. (Greenville, SC) was first dried at 120 °C in a vacuum oven for 6–8 h. The sulfonation reaction was performed by dissolving and reacting with 96% sulfuric acid (Fisher) at 20 °C. The initial concentration ratio of PEEK/sulfuric acid was maintained at 5/95 (wt./vol.) in all the experiments. After different lengths of reaction time (from 24 to 144 h), the sulfonated PEEK solution was then quenched in iced deionized water under mechanical agitation to recover the modified polymer. It was then repeatedly rinsed with deionized water and filtered to remove the residual sulfuric acid until the pH value of the washing water was above 5. The residual water in this recovered polymer was removed by drying the sample at 60 °C at vacuum for 24 h. The sulfonation degree and the ion exchange capacity (IEC) were determined by a titration method: 2–3 g SPEEK samples were first immersed into 1 M NaCl solution for 24 h and then were back titrated with 0.1 M NaOH using phenolphthalein as an indicator.

2.2. Membrane preparation

SPEEK membranes were prepared by dissolving the SPEEK sample in *N*,*N*-dimethylacetamide (DMAC) (99%, Aldrich) solvent to form a 5 wt.% solution. SPEEK membranes with different sulfonation degrees were cast by heating and evaporating the solvent from the solution in a glass Petri dish at 120 °C for 3 h. The membranes were obtained by adding deionized water to the surface and peeling the membranes from the dish. Different thickness membranes were obtained by controlling the solution amount and concentration in the casting step.

Nafion® membranes were also prepared by a solution casting procedure to compare with the SPEEK membranes. First, the commercial Nafion® solution (Solution Technology, Mendenhall, PA) was evaporated in a hood to remove the solvent (*iso*-propanol and water). Then the solid Nafion® was re-dissolved in *N*,*N*-dimethylacetamide (DMAC) (99%, Aldrich) solvent to get a 5 wt.% solution. The membrane casting procedure was the same as that of the SPEEK membranes.

2.3. Characterization of SPEEK

2.3.1. Thermogravimetry

A TGA2950 thermo-gravimetric analysis (TGA) instrument (TA Company, New Castle, Delware) was used to study the thermal stability behavior of SPEEK samples. The samples (∼10 mg) were heated in nitrogen from 25 to 900 °C with a scanning rate of 20 °C min^{-1}. Some samples were also heated in an air environment for comparison.

2.3.2. FTIR

Fourier transform infrared (FTIR) spectra were collected using a MAGNA-IR 560 Fourier Transform Infrared Spectrometer (Nicolet Instrument Corp., Madison, WI). PEEK samples was prepared by making KBr pellets composed of 50 mg of IR spectroscopic grade KBr and 1 mg polymer sample. Each SPEEK sample was prepared by casting a thin film of polymer onto a 13 mm × 2 mm KBr disc.

2.3.3. Water vapor uptake

Water vapor uptake properties of SPEEK membranes were measured with different water activities at room temperature (∼19 °C). Adsorption of water by the membrane was obtained in a closed equilibration vessel by suspending the membrane sample above a large volume of saturated salt solution, which was used to control the water activity in the vessel. The membrane sample was taken out from the vessel and weighed after 10 days equilibration. Membrane dry weight was measured after drying in vacuum at about 100 °C for 12 h. The water uptake was determined from the difference between wet and dry weights. Four saturated salts (LiCl, $MgCl_2$, NaBr and KBr) solutions and pure water were used in the vessel to control water activities. Saturation was assured by mixing a large excess (50%) of each salt with deionized water [24]. Water activity in each vessel with different saturated salt solution was monitored by a THGR228N digital hygrometer/thermometer (Fisher Scientific, Pittsburgh, PA).

2.4. Membrane electrode assemblies (MEAs)

2.4.1. MEAs preparation

MEAs were prepared by spraying catalyst ink containing carbon-supported catalyst and Nafion® in methanol onto the membrane. Forty weight percent Pt–Ru/C from E-TEK was

used as the anode catalyst. Pt/C (46.8 wt.%) from Tanaka (Tanaka, Kikinzoku Kogyo K.K. Japan) was used as the cathode catalyst. The composition of Nafion® in the catalyst was about 25 wt.% for both anode and cathode catalyst. The catalyst loading was about 0.7 mg catalyst metal cm^{-2} at both anode and cathode. After spraying the catalyst onto the membrane, the MEA was heat treated at 120 °C for 20 min. The active area for both the anode and cathode was 5 cm^2. The MEAs together with gas diffusion carbon paper (SIGRACET® GDL 10BB, SGL Technologies, Wiesbaden, Germany) applied on each side were tested in a single cell with 5 cm^2 flow channel area (FC05-01SP, Electrochem. Inc., Woburn, MA).

2.4.2. Membrane conductivity

Proton conductivity of membranes was determined from the membrane resistance measured by electrochemical impedance spectroscopy (EIS). The EIS measurements were carried out using a Solartron (Houston, TX) 1250 frequency response analyzer together with the Solartron 1287 electrochemical interface. The membrane resistance was measured in fuel cell hardware with humidified hydrogen applied to both the anode and cathode. The data was recorded using ZPLOT impedance software (Scribner Associates, Inc., Southern Pines, NC) which also controlled the experiments. EIS was conducted at the open circuit condition by applying a small alternating voltage (10 mV) and varying the frequency of the alternating voltage from 1×10^5 to 1 Hz.

2.4.3. MEAs fuel cell performance

MEA fuel cell performance was determined under ambient pressure with an in-house electrochemical test station that was equipped with a computer-controlled Scribner 890B load box (Scribner Associates Inc., Southern Pines, North Carolina). PEM fuel cell performance was evaluated at different cell temperatures (20–80 °C). Low relative humidity (42, 66% inlet RH) effects on cell performance were also studied at 80 °C. Hydrogen and oxygen were used as the anode fuel and cathode reactant respectively. To maintain constant utilization of fuel (34% for hydrogen) and oxidant (25% for oxygen), mass flow controllers were used to control gas flow rate with 3.4 stoichiometric H_2 flow at the anode and 4.0 stoichiometric O_2 flow at the cathode. Before the reactant gases entered the cell hardware, they were saturated with water in separate humidification bottles. The membrane resistance was also measured during performance testing using the current-interruption method, which permits direct measurement of the cell performance (IR-free performance) that is free from the polarization produced by the cell resistance.

2.4.4. Cyclic voltammetry (CV) and hydrogen crossover

Besides the fuel cell performance test, cyclic voltammetry (CV) and linear sweep voltammetry were used to compare or determine the electrochemical surface area (ECA) of the cathode electrode and the hydrogen crossover rate, respectively. CV experiments were carried out with a MEA in the fuel cell at 80 °C with various relative humidities (RHs). The hydrogen-fed anode was used as a reference and counter electrode. The cathode side was exposed to humidified nitrogen. Cyclic potential sweeps were carried out at a scan rate of 30 mV s^{-1} between 0.05 and 0.8 V versus RHE at 80 °C with RHs ranging from 100 to 66% and 42%, respectively. All the relative humidity mentioned in the experimental section is the inlet value. Hydrogen crossover was measured using the limiting current method by performing linear sweep voltammetry (LSV) with hydrogen flowing at the anode and nitrogen at the cathode. The cell voltage was scanned potentiodynamically at 4 mV s^{-1} from 0.05 to 0.55 V at 80 °C with various RHs (100, 66 and 42%). A Solartron 1286 potentiostat (Solartron Instrument, Houston, TX) was used to control the potential.

3. Results and discussion

3.1. Sulfonation of PEEK

Hydrophobic poly(ether ether ketone) (PEEK) is a thermostable polymer with an aromatic, non-fluorinated backbone, in which 1,4-disubstituted phenyl groups are separated by ether (–O–) and carbonyl (–CO–) linkages. To obtain ionic conductivity, sulfonic acid groups (–SO_3H) are functionalized onto the PEEK unit structure by a sulfonation reaction. The unit structure of PEEK and SPEEK is demonstrated in Fig. 1. Sulfonation is an electrophilic substitution reaction and substitution preferentially takes place in the high electron density site. Substitution will preferentially take place in one of the four positions of the aromatic ring between the ether bridges, as shown in the SPEEK repeat unit in Fig. 1, since the electron density of the other two aromatic rings in the repeat unit is relatively low due to the electron-attracting nature of the neighboring carboxyl group [25]. At room temperature with the concentrated sulfuric acid used as the solvent, there is at most one –SO_3H group attached to each repeating unit. In the sulfonation reaction, substitution is a

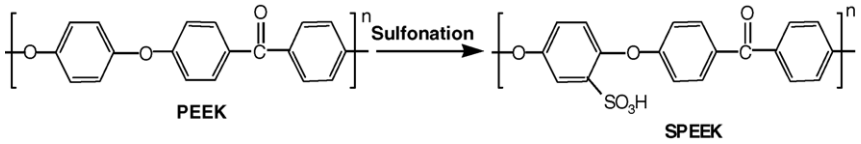

Fig. 1. Repeat unit of poly(ether ether ketone) and sulfonated poly(ether ether ketone).

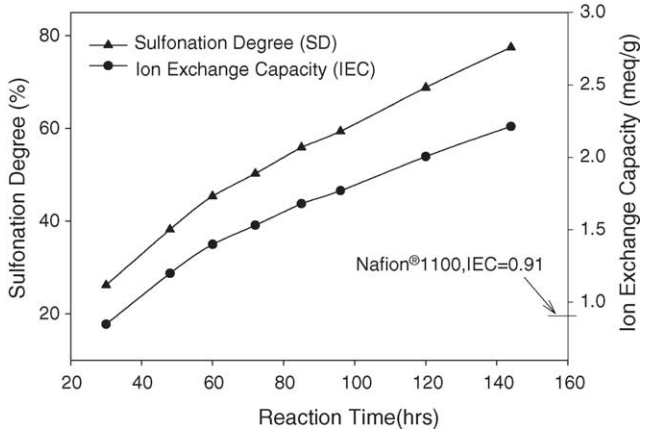

Fig. 2. Sulfonation degree (SD) and ion exchange capacity (IEC) of SPEEK as a function of sulfonation reaction time at room temperature.

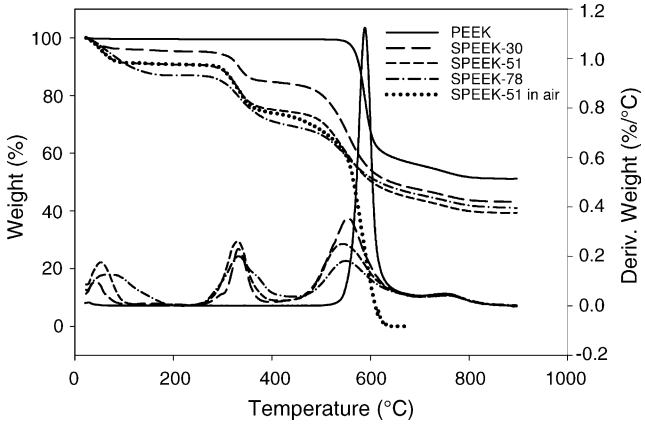

Fig. 3. Thermo-gravimetric analysis (TGA) of PEEK and SPEEK in nitrogen except where noted.

second-order reaction; the reverse reaction is neglected for high acid concentrations [25]. The sulfonation degree (SD) can be controlled by reaction time and temperature. The sulfonation degree (SD) is defined as the ratio of the molar number of sulfonated PEEK units to that of the total molar number of initial repeat units of PEEK. Eqs. (1) and (2) describe the determination of SD and IEC.

$$\mathrm{SD} = \frac{N_{\mathrm{PEEK\text{-}SO_3H}}}{N_{\mathrm{PEEK\text{-}SO_3H}} + N_{\mathrm{PEEK}}} \quad (1)$$

$$\mathrm{IEC} = \frac{N_{-\mathrm{SO_3H}}}{W_{\mathrm{sample}}} \times 1000 \quad (2)$$

Here, $N_{\mathrm{PEEK\text{-}SO_3H}}$ and $N_{-\mathrm{SO_3H}}$ are the molar number of sulfonated PEEK units and the molar number of sulfonate groups, respectively. N_{PEEK} is the molar number of unsulfonated PEEK units. W_{sample} represents the sample weight. According to the expressions of SD and IEC, the molar number, $N_{\mathrm{PEEK\text{-}SO_3H}}$, of the sulfonated PEEK unit (PEEK-SO_3H) in 1 g sulfonated PEEK copolymer is:

$$N_{\mathrm{PEEK\text{-}SO_3H}} = 0.001 \times \mathrm{IEC} \quad (3)$$

The molar number, of the PEEK unit in 1 g sulfonated PEEK copolymer is:

$$N_{\mathrm{PEEK}} = \frac{1 - 0.001 \times \mathrm{IEC} \times M_{\mathrm{PEEK\text{-}SO_3H}}}{M_{\mathrm{PEEK}}} \quad (4)$$

where $M_{\mathrm{PEEK\text{-}SO_3H}}$ and M_{PEEK} are the molecular weights of the PEEK-SO_3H unit and the PEEK unit, respectively. $M_{\mathrm{PEEK\text{-}SO_3H}} = 368$ Da and $M_{\mathrm{PEEK}} = 288$ Da [25].

The PEEK was sulfonated at room temperature for different reaction times ranging from 30 to 144 h to produce different SD SPEEKs. The SD and IEC of each SD SPEEK polymers were determined by the titration results and the equations above. Fig. 2 shows the SD and IEC of SPEEK as a function of sulfonation reaction time. IEC of Nafion® 1100 is also noted in Fig. 2 as comparison. It is clear that the SD and IEC of SPEEK continuously increase with increasing sulfonation reaction time. With a reaction time of 48 h, the SD is 38% and the IEC is 1.2, which is higher than Nafion® 1100 ($\mathrm{IEC_{Nafion®\ 1100}} = 0.91$).

3.2. Thermal stability of SPEEK

Fig. 3 shows the thermo-gravimetric analysis results of PEEK and SPEEKs with different degrees of sulfonation. PEEK demonstrates excellent thermal stability with a decomposition temperature higher than 500 °C. For SPEEK, after dehydration of the membrane, no further weight loss is observed until degradation of the sulfonic groups commences at around 260 °C. The decomposition of the SPEEK is observed above 450 °C. The thermal property of SPEEK is satisfactory for the operating requirement of PEM fuel cell. The weight loss due to dehydration increases with the higher degree of sulfonation, indicating that more water was taken up for higher SD SPEEK membranes. Here SPEEK-30 represents SPEEK membranes with a 30% sulfonation degree, similarly for SPEEK-51 and SPEEK-78. To investigate thermal stability of SPEEK under an oxygenated environment, a TGA of SPEEK-51 performed in air instead of nitrogen is also shown in Fig. 3. There is little difference before 400 °C in the weight percent loss curves, indicating degradation by oxidation is very small in this temperature range. At temperatures higher than 400 °C oxidation is increased and all of the polymer material is consumed when the temperature reaches 670 °C.

3.3. FTIR study

The FTIR spectra of PEEK and SPEEK with different sulfonation degrees are shown in Fig. 4. The new absorption bands at 1020, 1076 and 1247 $\mathrm{cm^{-1}}$ of SPEEK can be assigned to the symmetric and asymmetric stretching vibrations of the sulfonic acid group. The aromatic C–C band at 1486 $\mathrm{cm^{-1}}$ for PEEK is observed to split into two peaks at 1471 and 1492 $\mathrm{cm^{-1}}$ for SPEEK, due to the new substitute from sulfonation [26].

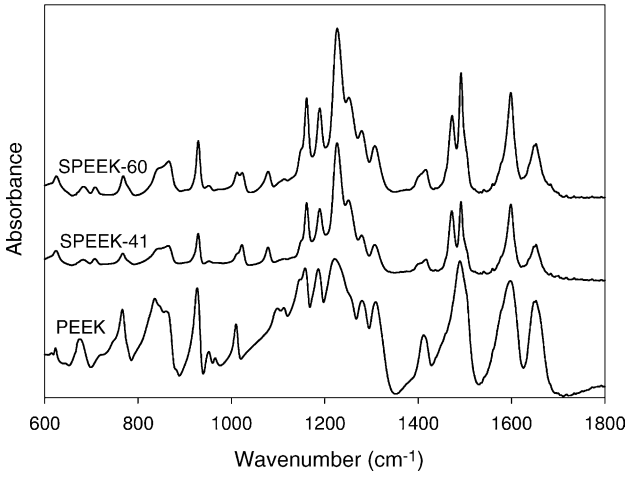

Fig. 4. FTIR spectra of PEEK and SPEEK.

3.4. Water vapor uptake

Water uptake from the vapor phase is likely to be the principal mode of external hydration of the membrane in a PEM fuel cell. Sorption of water vapor of controlled activity by Nafion® and SPEEK membranes with various sulfonation degrees was investigated in this study. Membrane samples were suspended above various aqueous saturated salt solutions. The relationship between water activity measured by the hydrometer and the type of saturated salt solution is listed in Table 1. Water activities over the range of 0.12–0.98 can be accessed using different saturated salt solutions at room temperature.

The water vapor sorption curves for Nafion® and SPEEK membranes with various SD are shown in Fig. 5. Fig. 5(a) presents the weight uptake ratio of the membrane in percent of dry weight by absorbing water vapor at each water vapor activity. It shows that membranes uptake more water with increasing water vapor activity. For SPEEK membranes, the water uptake increases with increasing sulfonation degree. The water uptake of a Nafion® membrane in water vapor is lower than SPEEK membranes with 51% or larger sulfonation degrees. Fig. 5(b) compares the value of λ, $\lambda = N_{H_2O}/N_{-SO_3H}$, of each membrane. Here λ denotes the molar number of water taken up by each mole of sulfonic acid group. Fig. 5(b) indicates that for SPEEK membranes, λ values at each water vapor activity increase with increasing sulfonation degree. SPEEK membranes with sulfonation degrees higher than 60% have higher λ value than Nafion® membranes. From Fig. 5(b), with increasing water vapor activity, water sorption can be discriminated in two regions: (1) a low vapor activity region, $\alpha_{H_2O} < 0.75$, characterized by a relatively small increase in water content with water vapor activity and (2) a high vapor activity region, $\alpha_{H_2O} = 0.75$–1.0, characterized by steeper increase of water content with water activity. The results are similar to those reported by Zawodzinski et al. [27], who investigated the isopiestic sorption curve for Nafion® 117 membranes at 30 °C. According to Zawodzinski et al., region (1) corresponds to uptake of water by the ions in the membrane, while region (2) corresponds to water which fills the (submicro) pores and swells the polymer. Fig. 5(b) also shows that the slope of region (2) becomes steeper with increasing sulfonation degree, indicating more serious membrane swelling for higher SD SPEEK membranes.

Table 1
Water vapor activities with different saturated salt solutions in the vessel

Salt	LiCl	$MgCl_2$	NaBr	KBr	H_2O
Water vapor activity	0.12	0.34	0.58	0.79	0.98

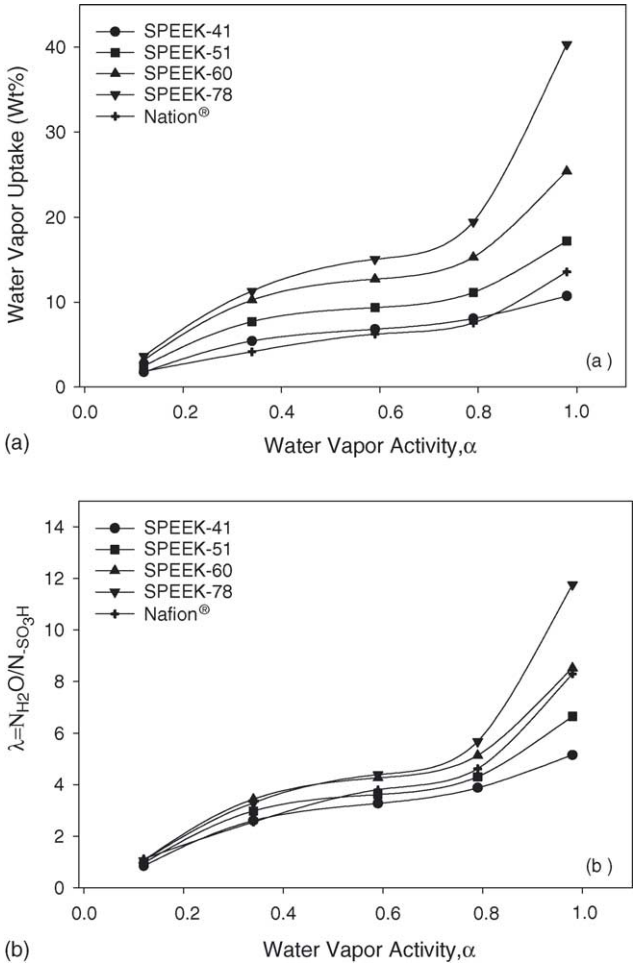

Fig. 5. Water vapor uptake properties of SPEEK and Nafion® membranes as a function of water vapor activity, α. (a) Weight percent vs. α; (b) λ vs. α.

3.5. Membrane proton conductivity

The proton conductivity, σ, of membranes in the through-plane direction was calculated from the impedance data using the relation $\sigma = L/RA$, where L and A are the thickness and face area of the membrane sample, respectively, and R was derived from the intersection of the high frequency semi-circle on the complex impedance plane with the real (Z) axis.

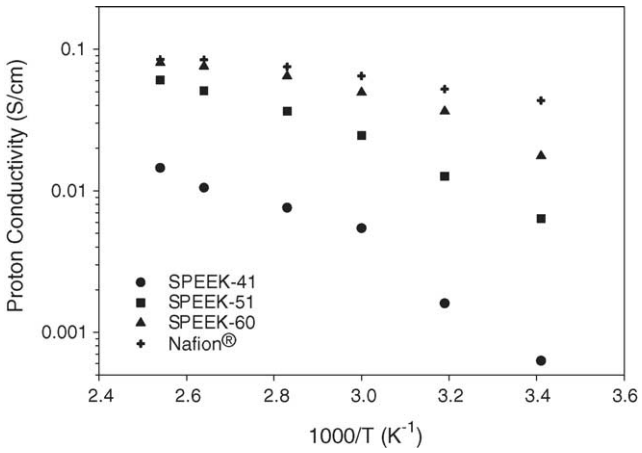

Fig. 6. Arrhenius plots of proton conductivity of SPEEK membranes with different sulfonation degrees as a function of temperature.

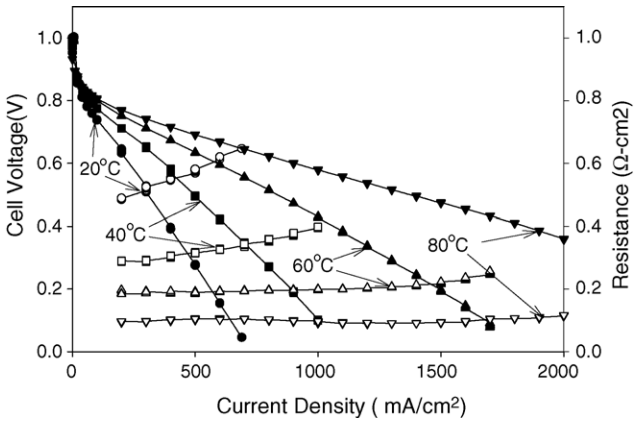

Fig. 8. PEM fuel cell performance and cell resistance with a SPEEK-51 membrane at different cell temperatures and 100% relative humidity. H_2/O_2 at ambient pressure.

The proton conductivity of Nafion® and SPEEK membranes with sulfonation degrees between 41 and 60% under fully humidified condition is reported in Fig. 6 as Arrhenius plot. Unlike Nafion®, the conductivity of SPEEK membranes does not really follow Arrhenius behavior as evidenced by the nonlinear decrease in logarithm conductivity with reciprocal temperature. Proton conductivity of all SPEEK membranes in this sulfonation degree range (41–60%) is lower than Nafion®. The proton conductivity of SPEEK membranes significantly increases with increasing sulfonation degree. The conductivity of SPEEK-51 and SPEEK-60 membranes above 40 °C is higher than 0.01 S cm^{-1} and within the same magnitude as Nafion®. At temperatures higher than 80 °C, the conductivity values of SPEEK-60 are close to that of Nafion®: $\sigma = 0.064$ for SPEEK-60 and $\sigma = 0.075$ for Nafion® at 80 °C; $\sigma = 0.080$ for SPEEK-60 and $\sigma = 0.084$ for Nafion® at 120 °C.

The variation of the conductivity of SPEEK-51 and Nafion® membranes with relative humidity at 80 °C is compared in Fig. 7. For the SPEEK-51 membrane, the conductivity curve as a function of RH shows a much steeper slope than that of the Nafion® membrane, indicating a larger variation of conductivity with RH.

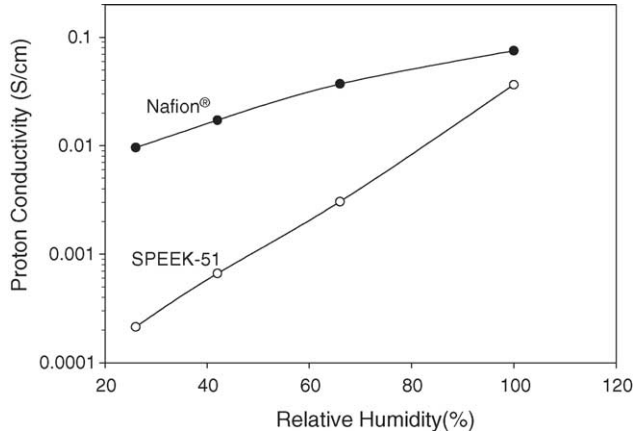

Fig. 7. Relative humidity effects on proton conductivity of Nafion® and SPEEK-51 membranes at 80 °C.

3.6. MEAs performance in PEM fuel cells

SPEEK membranes with certain sulfonation degrees have reasonable proton conductivities as discussed above. Membrane electrode assemblies (MEAs) based on SPEEK-51 membranes were developed and studied in H_2/O_2 fuel cells. For fuel cell use, thin membranes have a significant advantage in terms of lower resistance, improved water management of the membrane as well as lower cost of materials. In this study, 25 μm thick SPEEK membranes were prepared and fuel cell performance tested. Fig. 8 shows MEA fuel cell performance and cell resistance with a SPEEK-51 membrane at different cell temperatures and 100% relative humidity. Humidified H_2 and O_2 under ambient pressure were applied to the cell anode and cathode, respectively. At 80 °C, the cell shows very good performance with cell voltages of 0.95, 0.77 and 0.72 V at current densities of 0 (open circuit), 200 and 400 mA cm^{-2}, respectively. As cell temperature decreases, the cell resistance increases and the cell performance decreases as well. As cell temperature decreases from 80 to 60 °C, 40 and 20 °C, the cell voltage at 200 mA cm^{-2} decreases from 0.77 V at 80 °C to 0.75 V at 60 °C, 0.71 V at 40 °C and 0.63 V at 20 °C. Meanwhile, cell resistances at 200 mA cm^{-2} measured by current interrupt increased from 0.084 to 0.16 Ω cm^2, 0.28 and 0.48 Ω cm^2, respectively.

Fig. 8 also presents the cell resistances measured by current interrupt as a function of current density at each temperature condition. At 80 °C, the values of cell resistance are relatively constant in the current density range from 200 mA cm^{-2} to 2000 mA cm^{-2}, although the cell resistance increases slightly when the current density is higher than 1600 mA cm^{-2}. At 60 °C, the cell resistance increases with current density more than that at 80 °C when the current density is higher than 1300 mA cm^{-2}. At the 40 and 20 °C

conditions, cell resistance increases dramatically when the current density is higher than 400 mA cm^{-2} and 200 mA cm^{-2}, respectively. At 20 °C, cell resistance increases drastically with current density. The increase in cell resistance with current density is caused by the water distribution in the membrane due to the interplay of electro-osmotic drag transporting water toward the cathode and the back transport of water to the anode [27,28]. During fuel cell operation, with the proton conducted from the anode to cathode, water can be dragged by forming H_3O^+ and moved from the cell anode to cathode. On the other hand, the cell cathode has a higher water concentration, which drives water diffusion from the cathode to the anode due to a concentration gradient and capillary forces. The amount of water transported by electro-osmotic drag and back diffusion is dependent on current density, membrane properties and thickness. With increasing current density, the increased proton flux carries a large amount of water to the cathode. At very high current densities, the water back diffusion flux from the cathode to anode is not sufficient to make up for the water lost at the cell anode, so the anode side of the membrane dries out causing a large membrane resistance. According to Zawodzinski et al. [27] and Buchi et al. [28], the back diffusion flux of water is directly proportional to the water diffusion coefficient or the water permeability of the membrane, which is determined by the local water content in the membrane. The steep slope of cell resistance with current density at 20 °C indicates that the back diffusion of water is very sensitive to current density, due to a small water diffusion coefficient at 20 °C. The cell resistance becomes less dependent on current density as the cell temperature increases, indicating both an increased water diffusion coefficient and higher water content at higher temperature.

The effect of relative humidity on fuel cell performance was also studied using SPEEK-51 membranes. Fig. 9(a) compares cell performance at 80 °C with 100% RH, 66% RH, 42% RH and then a repeat test at 100% RH. The cell voltage at 200 mA cm^{-2} significantly decreases from 0.77 V at 100% RH to 0.46 V at 66% RH. At 42% RH condition, the cell was shut down before reaching a current density of 100 mA cm^{-2} due to a very low cell voltage. The repeat test at 100% RH shows similar performance as the first test at 100% RH, indicating the cell performance can be recovered after suffering a dry environment at lower RH tests. Fig. 9(b) shows the IR-Free voltage profiles at different relative humidity conditions. The cell voltage was compensated by the cell resistance as measured by current interrupt (the cell resistance at 42% RH was measured by electrochemical impedance). Even with IR correction, the IR-Free cell voltages at lower RH are still much lower than that at 100% RH. The lower RH not only increases the membrane resistance which leads to IR losses, but also dries out the catalyst layer which decreases the catalyst utilization. The fuel cell performance decrease at lower RH conditions is due to the combined effects of the lower proton conductivity of dry membrane and catalyst layer, and the lower catalyst utilization induced by the ion immovability

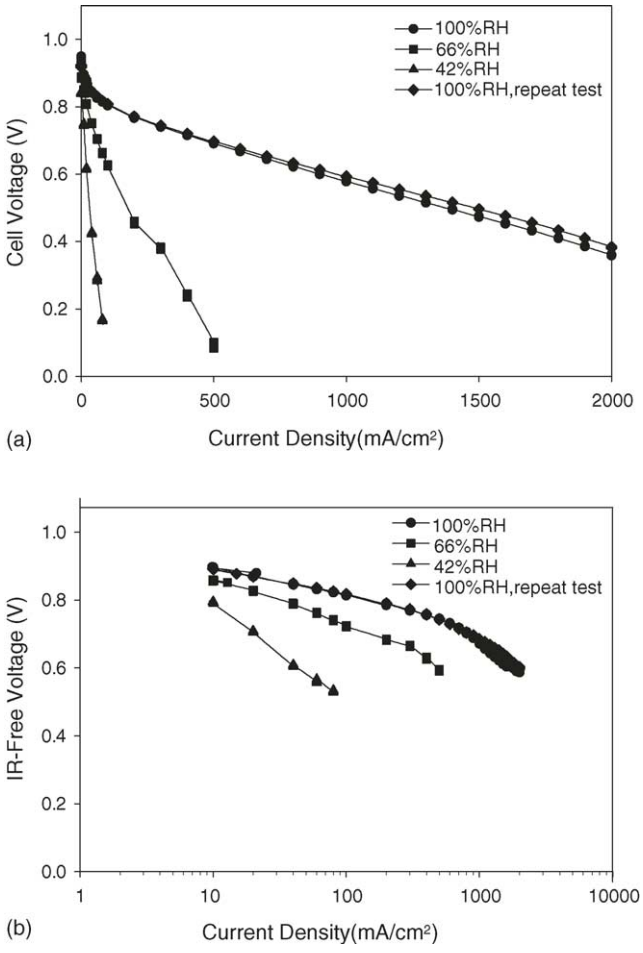

Fig. 9. Relative humidity effects on PEM fuel cell performance with a SPEEK-51 membrane in a H_2/O_2 cell at 80 °C under ambient pressure. (a) Cell voltage vs. current density; (b) IR-free voltage vs. current density.

in the membrane and the catalyst layer. In addition, the lower oxygen permeability in the proton conductor in the cathode catalyst layer at lower RH might contribute further to the performance loss [29].

3.7. Results of CV and hydrogen crossover

As shown in Fig. 10(a), cyclic voltammetries (CV) were performed to the MEA at 80 °C with three relative humidity conditions. The peaks at potential range of 0.1–0.4 V are associated with hydrogen adsorption/desorption on the Pt catalyst active surface. The shapes of voltammograms are different at those three RH conditions. At 100% RH condition, two large peaks appear at 0.13 and 0.24 V, which are caused by the hydrogen adsorption on different crystal planes of Pt. In contrast, the size of those two peaks significantly decreases at 66% RH condition, and only one broad adsorption peak is observed at 42% RH condition. Electrochemically active area of the catalyst (ECA) can be estimated based on the relationship between the surface area and the hydrogen adsorption charge on the electrode determined from the CV measurement, hydrogen adsorption charge on a smooth Pt electrode

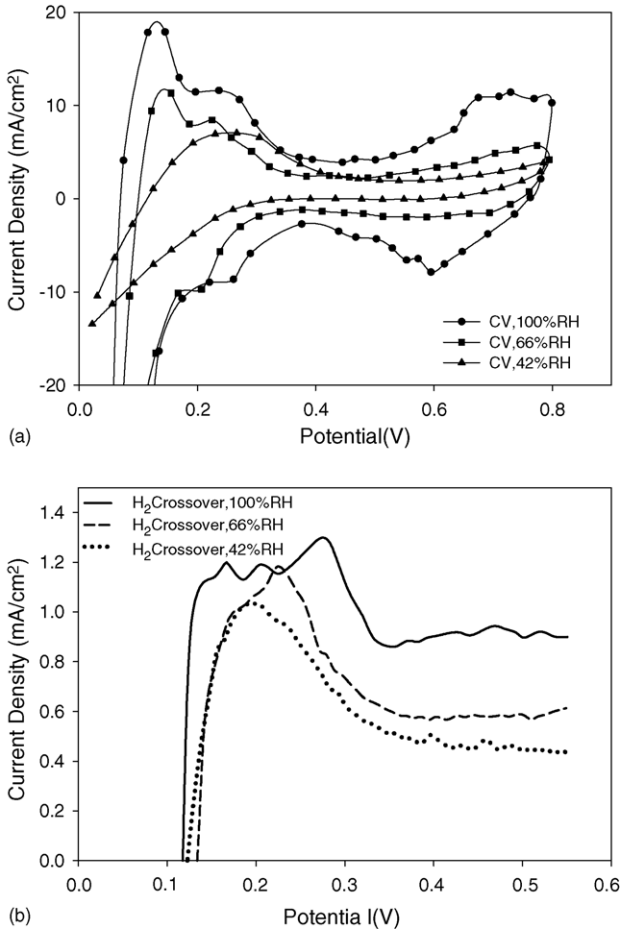

Fig. 10. (a) Cyclic voltammetries and (b) H_2 crossovers by potentiodynamic of PEM fuel cell with a SPEEK-51 membrane at 80 °C with different relative humidities. H_2/N_2 under ambient pressure.

of 210 μC cm^{-2} Pt, and the Pt loading in the catalyst layer. The ECA of the cathode electrode is calculated by using the Eq. (5) below.

$$\text{ECA}\,(\text{m}^2\,\text{g}^{-1}\,\text{Pt}) = \frac{\text{Charge}\,(\mu\text{C}\,\text{cm}^{-2}) \times (10^{-4}\,\text{m}^2\,\text{cm}^{-2})}{(210\,\mu\text{C}\,\text{cm}^{-2}\,\text{Pt}) \times \text{Catalyst loading}\,(\text{g Pt}\,\text{cm}^{-2})} \quad (5)$$

ECA of the cathode electrode obtained according to Eq. (5) is 89, 53 and 38 m^2 g^{-1} Pt for 100, 66 and 42% RH condition, respectively. When compared to the total surface area of 134 m^2 g^{-1} Pt (provided by the manufacturer), the catalyst utilization is 67, 40 and 28%, respectively, for the conditions with those three relative humidities. To be electrochemically active in the reaction, the catalyst has to have the access to the electron and proton conductor and the reactant gas. The smaller catalyst active area or the lower catalyst utilization at lower RH conditions is caused by the proton immovability in the catalyst layer, due to the dehydration effect at low humidity. Although the catalysts are in contact with dehydrated proton conductor and reactant gas, the immobility of the protons prevents the reaction from occurring. Therefore, it is obvious that the lower catalyst utilization at lower RH causes additional performance loss.

Hydrogen crossover is the undesirable diffusion of hydrogen through the membrane from the anode side to the cathode side where hydrogen reacts chemically with oxygen or oxygen in the air to form water. Hydrogen crossover lowers fuel efficiency and if too much hydrogen reaches the cathode, hot spots may occur that destroy the MEA and cause safety issues. This is why low H_2 crossover is required for fuel cell operation. In this study, the limiting current method using linear sweep voltammetry (LSV) technique was applied to evaluate the hydrogen crossover of the SPEEK-51 membrane at 80 °C with various relative humidities. Fig. 10(b) shows the result of LSV of a MEA with 25 μm thick SPEEK-51 membrane at 80 °C with various relative humidities. Low potential scan rate (4 mV) was used during the LSV measurement to minimize the effect of double layer capacitance charge. Hydrogen crossover was qualitatively determined from Fig. 10(b) by the plateau current density at higher potential (0.45 V) where the current obtained was primarily limited by the hydrogen transport rate through the tested membrane. Hydrogen oxidation pseudo-capacitance is apparent at potentials lower than 0.35 V even with such a low value of potential scan rate. Determined from the plateau in Fig. 10(b), the limiting current is about 0.85, 0.6 and 0.45 mA cm^{-2} respectively at the relative humidity conditions of 100, 66 and 42%, showing a decreasing value in sequence. The difference of hydrogen crossover limiting current of the SPEEK-51 membrane at these three relative humidity conditions shows the similar trend as that of Nafion® membrane [30,31]. Nevertheless, at all operating conditions, the hydrogen crossover rate remains low, and has little effect to the performance losses at lower relative humidity conditions.

4. Conclusion

A series of SPEEKs were prepared by sulfonation of PEEK with concentrated sulfuric acid at room temperature with the sulfonation degree controlled by varying the reaction time. Thermo-gravimetric analysis shows good thermal stability of SPEEKs with the degradation temperature higher than 260 °C. Water vapor uptake of SPEEK membranes increases with increasing sulfonation degree. The water uptake of the Nafion® membrane in water vapor is lower than SPEEK membranes with sulfonation degree of 51% or higher. SPEEK membranes with sulfonation degree higher than 60% have higher λ values, $\lambda = N_{H_2O}/N_{-SO_3H}$, than that of Nafion®. With increasing water vapor activity, two distinct water sorption regions were observed: the low water vapor activity region ($\alpha_{H_2O} < 0.75$) where there is low water content increasing; and high water vapor activity region ($\alpha_{H_2O} < 0.75$–1) where there is high water content increasing. The slope of the high water vapor activity region is steeper for SPEEK membranes with higher sulfonation

degrees, which indicates a higher membrane swelling. Proton conductivity of SPEEK membranes increases with increasing sulfonation degree. SPEEK membranes with sulfonation degrees higher than 50% show proton conductivity values higher than 0.01 S cm^{-2} at temperatures higher than 40 °C, which is within the same magnitude as Nafion®. The conductivity decreases more at lower RH for the SPEEK-51 membrane than for the Nafion® membrane. Fuel cell performance at increasing temperature and 100% RH shows decreased cell resistance and increased cell performance. MEAs with the SPEEK-51 membrane show very good performance at 80 °C, 100% RH and ambient pressure, which indicates potential application of SPEEK membranes for fuel cells. The cell resistance becomes much more dependent on current density as the cell temperature decreases. Fuel cell performance greatly decreases with a decreasing in relative humidity. Behavior of cyclic voltammetry (CV) and hydrogen crossover of the fuel cell has significant dependence on relative humidity. Lower RH led to higher voltage losses due to dehydration of membrane and catalyst layer, and lower catalyst utilization induced by lower proton conductivity in the membrane and catalyst layer.

Acknowledgement

The authors greatly acknowledge the generous gift of PEEK powder (450PF) from Victrex US Inc. (Greenville, SC).

References

[1] S. Gottesfeld, T.A. Zawodzinski, in: R.C. Alkire, H. Gerischer, D.M. Kolb, C.W. Tobias (Eds.), Advances in Electrochemical Science and Engineering, vol. 5, Wiley-VCH, Weinheim, 1997, p. 220.
[2] G. Inzelt, M. Pineri, J.W. Schultze, M.A. Vorotyntsev, Electrochim. Acta 45 (2000) 2403.
[3] M. Higuchi, N. Minoura, T. Kinoshita, Chem. Lett. 227 (1994).
[4] K.D. Kreuer, J. Membr. Sci. 185 (2001) 29.
[5] J. Kerres, A. Ullrich, T. Haring, M. Baldauf, U. Gebhardt, W. Preidel, J. New Mater. Electrochem. Syst. 3 (2000) 229.
[6] D.J. Jones, J. Roziere, J. Membr. Sci. 185 (2001) 41.
[7] K.D. Kreuer, J. Membr. Sci. 185 (2001) 3.
[8] M. Rikukawa, K. Sanui, Prog. Polym. Sci. 25 (2000) 1463.
[9] F. Wang, M. Hickner, Y.S. Kim, T.A. Zawodzinski, J.E. McGrath, J. Membr. Sci. 197 (2002) 231.
[10] Y.-L. Ma, J.S. Wainright, M.H. Litt, R.F. Savinell, J. Electrochem. Soc. 151 (2004) A8.
[11] J.T. Wang, R.F. Savinell, J. Wainright, M. Litt, H. Yu, Electrochim. Acta 41 (1996) 193.
[12] B. Bauer, D.J. Jones, J. Roziere, L. Tchicaya, G. Alberti, M. Casciola, L. Massinelli, A. Peraio, S. Besse, E. Ramunni, J. New Mater. Electrochem. Syst. 3 (2000) 93.
[13] G.P. Robertson, S.D. Mikhailenko, K. Wang, P. Xing, M.D. Guiver, S. Kaliaguine, J. Membr. Sci. 219 (2003) 113.
[14] G. Alberti, M. Casciola, L. Massinelli, B. Bauer, J. Membr. Sci. 185 (2001) 73.
[15] B. Yang, A. Manthiram, Electrochem. Solid-State Lett. 6 (11) (2003) A229.
[16] P. Xing, G.P. Robertson, M.D. Guiver, S.D. Mikhailenko, K. Wang, S. Kaliaguine, J. Membr. Sci. 229 (2004) 95.
[17] L. Jorissen, V. Gogel, J. Kerres, J. Garche, J. Power Sources 105 (2002) 267.
[18] Carmen Manea, Marcel Mulder, J. Membr. Sci. 206 (2002) 443.
[19] W. Cui, J. Kerres, G. Eigenberger, Sep. Purif. Technol. 14 (1998) 145.
[20] B. Bonnect, D.J. Jones, J. Roziere, L. Roziere, L. Tchicaya, G. Alberti, M. Casciola, L. Massinelli, B. Bauer, A. Peraio, E. Ramunni, J. New Mater. Electrochem. Syst. 3 (2000) 87.
[21] M.L. Ponce, L. Prado, B. Ruffmann, K. Richau, R. Mohr, S.P. Nunes, J. Membr. Sci. 217 (2003) 5.
[22] S.P. Nunes, B. Ruffmann, E. Rikowski, S. Vetter, K. Richau, J. Membr. Sci. 203 (2002) 215.
[23] S.M.J. Zaidi, S.D. Mikhailenko, G.P. Robertson, M.D. Guiver, S. Kaliaguine, J. Membr. Sci. 173 (2000) 17.
[24] M.L. Pollio, D. Kitic, S.L. Resnik, Lebensm.-Wiss. u –Technol. 29 (1996) 376.
[25] R.Y.M. Huang, P. Shao, C.M. Burns, X. Feng, J. Appl. Polym. Sci. 82 (2001) 2651.
[26] J. Devaus, D. Delimony, D. Daoust, R. Legras, J.P. Mercier, Polymer 26 (1985) 1994.
[27] T.A. Zawodzinski Jr., C. Derouin, S. Radzinski, R.J. Sherman, V.T. Smith, T.E. Springer, S. Gottesfeld, J. Electrochem. Soc. 140 (1993) 1041.
[28] F.N. Buchi, G.G. Scherer, J. Electrochem. Soc. 148 (2001) A183.
[29] K. Broka, P. Ekdunge, J. Appl. Electrochem. 27 (1997) 117.
[30] T. Sakai, H. Takenaka, E. Torikai, J. Electrochem. Soc. 133 (1986) 88.
[31] T. Sakai, H. Takenaka, N. Wakabayashi, Y. Kawami, E. Torikai, J. Electrochem. Soc. 132 (1985) 1328.